

Surfactant/Polymer Assemblies. 1. Surfactant Binding Properties

David P. Norwood,[†] Edson Minatti, and Wayne F. Reed*

Department of Physics, Tulane University, New Orleans, Louisiana 70118

Received September 5, 1997; Revised Manuscript Received February 6, 1998

ABSTRACT: The binding characteristics of aggregates formed between neutral polymer (PVP) and anionic surfactant (SDS) are explored by light scattering. As added SDS binds to PVP polymers, the mass increase of the scattering aggregates is reflected in higher scattered intensity, so long as electrostatic interactions due to the SDS charge (as reflected in the second virial coefficient, A_2) are suppressed by high ionic strength. Although there is an equilibrium between bound and free SDS, the majority of the scattering observed is due to SDS/PVP aggregates. These aggregates appear to consist of single PVP polymer chains with multiple bound SDS micelle-type structures. Attempts are made to quantify the binding of SDS to PVP in terms of the binding energy and binding volume, using both a model of scattering from multicomponent systems and a model of the thermodynamics of the binding process. Additionally, the saturation of PVP with SDS allows us to determine the stoichiometry of the SDS/PVP aggregation and suggest a physical cause for the saturation.

Introduction

Surfactant and polymer mixtures in solution are used for industrial applications in the medical, cosmetic, food, paint, enhanced oil recovery, and other sectors. Sodium dodecyl sulfate (SDS) interacts strongly with neutral polymers, such as poly(ethylene oxide) (PEO) and poly(vinyl pyrrolidone) (PVP). These systems have been extensively studied by viscometry,¹ surface tension,^{2,3} dialysis,⁴ conductivity,^{5,6} potentiometric measurements,⁷ NMR spectroscopy,^{8,9} light and neutron scattering,¹⁰ electrophoretic light scattering,^{11,12} fluorescence spectroscopy,^{13,14} and kinetic probes.^{15,16}

Several plausible scenarios for the mechanism of interaction between neutral polymers and charged surfactants have been proposed. These models can be divided into three main groups: (a) attachment of individual surfactant monomers to the polymers chain;^{2,17–19} (b) attachment of micelle-like aggregates of the surfactant to the polymer chain;^{5,11,12,20,21} (c) a combination of scenarios a and b, whereby monomers begin to bind, forming “nuclei” for further binding of micelles.^{22–24}

It is known that a critical surfactant concentration exists for the interaction between polymers and surfactants (“critical aggregation concentration” or CAC). This contradicts mechanism a, which allows monomers to successively attach to the polymer without an abrupt transition. There is substantial evidence to support mechanism b. NMR results^{8,9} indicate that interactions in PEO–SDS aggregates involve association of the polymer with micelle-like aggregates of the surfactant: the environment of the surfactant alkyl group is similar to that in ionic micelles. It also shows that the interaction occurs in the headgroup or in its neighborhood.

Schwuger²⁵ suggested that the “interactions are probably due to a partially positive charge transfer to the ether oxygen group and, consequently, an increased attraction of the hydrophilic group of the anionic surfactant.” This postulate would explain the absence of

interaction between cationic surfactants and neutral polymers such as PEO and PVP. Schwuger also showed that, with increasing pH, the amount of surfactant bound to the polymer decreases. In his interpretation, the increase of pH, leading to a reduction of the partial positive charge of PEO molecules, decreases the tendency to aggregate formation.

Dubin et al.^{11,12} also assume that the counterions play a role in these interactions, simultaneously coordinating with the polymer oxygens and being electrostatically bound to the micelle. The neutral polymer, when coordinated with the cation in the double layer, becomes a “pseudopolycation”,¹⁵ forming aggregates with the anionic micelles. Ion selective electrode and ultrafiltration experiments²⁶ have shown that significant binding is verified for sodium, potassium, rubidium, and cesium chlorides on PEO chain (in the absence of any surfactant), creating a net positive potential that attracts the anions to the vicinity of the polymer chain. This model is discussed further in the second part of this work.

The idea of micelle-like aggregation is also supported by Gilanyi et al.⁷ Their results in potentiometric experiments showed that the standard free energy change of the transfer of DS^- ions into surfactant aggregate subunits is very close to that of micelle formation. They also reported that the energy of interaction between aggregates in the same polymer chain seems to be insignificant compared to that of aggregate formation, which is consistent with our results.

Engberts et al.²⁷ reported that both the nature of the surfactant headgroup and the number of carbons in the surfactant tail have an effect on the polymer–surfactant interaction. They showed that SDeP (sodium decyl phosphate) has almost no interaction with PEO, while the SDeS (sodium decyl sulfate) does interact. They concluded that the increase of the alkyl chain length of the surfactant enhances polymer–micelle interaction.

Despite uncertainties about the structure and formation mechanism of polymer–surfactant aggregates, estimates exist of important parameters, such as micelle aggregation number, degree of ionization, and effect of

* Author for correspondence.

[†] Present address: Dept. of Chemistry and Physics, Southeastern Louisiana University, Hammond LA 70402.

ionic strength. These aggregates are similar to aqueous micelles but are smaller and have a higher degree of ionization. Somasundaram et al.^{28,29} estimated the aggregation number for several salts concentrations using fluorescence techniques. They did not see any effect of increasing ionic strength on the size of the bound aggregate. The only parameter affected was the number of bound surfactants per polymer chain. They estimated the aggregation number for PEO–SDS aggregates as about 30 in 0.50 M NaCl. Lissi et al.³⁰ found aggregation numbers of 35 ± 5 in the absence of salt and 46 ± 5 at 0.1 M NaCl. Gilanyi et al.⁷ found evidence for an increase of the aggregation number for PVA (poly(vinyl alcohol))–SDS aggregates with increasing ionic strength. They found an aggregation number of 12 in the absence of salt and one around 45 ± 5 in 0.1 M NaNO₃. Dubin et al.¹² also reported that the amount of LDS (lithium dodecyl sulfate) bound per chain of PEO increases with increasing ionic strength, as does the electrophoretic mobility.

It is the aim of this work and the companion paper to determine the degree to which the behavior of these assemblies, consisting of SDS micelles attached to isolated polymer molecules, actually resembles that of true polyelectrolytes and to make structural deductions about the assemblies themselves, including the binding fraction, energy, and mechanism. The current paper will focus on binding effects, while the polyelectrolyte properties will be addressed in a companion paper. Because surfactant molecules can assemble into micelles in a way which depends on both their concentration and ionic strength and can also interact with the neutral polymers, the situation is considerably more complicated than that for polymeric polyelectrolytes.

Materials and Methods

SDS was from Sigma Chemical Co. (No. L-6026), PEO was from Aldrich Chemical CO. (No. 30,902-8, nominal $M_n = 10\,000$, and No. 20,245-2, nominal $M_n = 8000$), and PVP was from Aldrich (No. 43,719-0, nominal $M_w = 1\,300\,000$, and No. 86,645-2, nominal $M_w = 10\,000$).

The majority of experiments were performed on high molecular mass PVP for two reasons. The first is that the saturation point is higher for a large mass polymer, permitting us to measure a larger mass enhancement obtained over a larger range of SDS concentration. This gives a larger signal-to-noise in the measured mass enhancement under conditions which minimize the effects of the second virial coefficient A_2 (high ionic strength and low concentration). The second reason relates to the polyelectrolyte properties and is addressed in the accompanying paper. Briefly, at low ionic strength and high concentration (in contrast to the regime discussed above), the high molecular weight allows the effects of A_2 to be more clearly measured, since the term $2A_2cM_w$ (which, in the limit $q = 0$, is the ratio of the second term to the first term on the right-hand side of eq 4 below), can be on the order of, or larger than 1. The effect on A_2 of electrically charging PVP by association with SDS and of varying the ionic strength C_s will be addressed in the accompanying work.

A size exclusion chromatography (SEC) analysis of PVP was made on a system consisting of a Hewlett-Packard 1100 isocratic HPLC pump, an Erma ERC-7522 refractometer, a Wyatt Dawn-F light scattering photometer in "flow mode", and a homemade single capillary viscometer. The columns were Shodex SB805HQ followed by SB806HQ, whose packing material is poly(hydroxymethyl methacrylate). A critical analysis of the performance of this system has been made recently, with particular attention to the viscometric detector portion.³¹

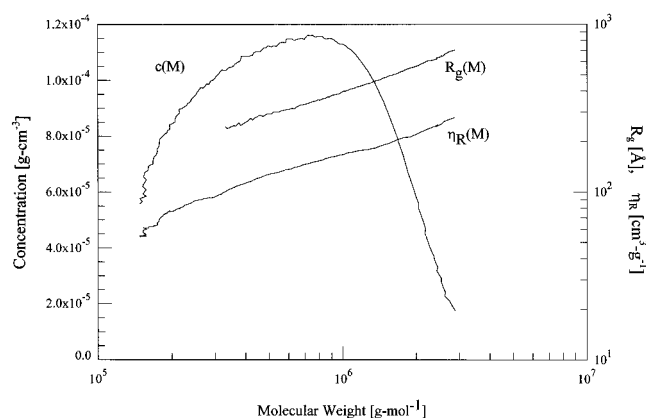


Figure 1. Multidetector size exclusion chromatography results for the PVP used, plotted as a function of molecular weight, M . Shown are concentration, $C(M)$, in g/mL; radius of gyration, $R_g(M)$ in angstroms, and intrinsic viscosity, $[\eta](M)$, in mL/g.

Table 1. Properties of PVP from SEC^a

parameter	value
number average molecular mass M_n (10^3 g mol ⁻¹)	447 ± 29
weight average molecular mass M_w (10^3 g mol ⁻¹)	801 ± 47
Z average molecular mass M_z (10^3 g mol ⁻¹)	1310 ± 65
polydispersity M_w/M_n	1.791 ± 0.016
polydispersity M_z/M_w	1.636 ± 0.017
number average radius of gyration $R_{g,n}$ (Å)	301 ± 37
weight average radius of gyration $R_{g,w}$ (Å)	381 ± 23
Z average radius of gyration $R_{g,z}$ (Å)	475 ± 18
number average apparent persistence length $L'_{T,n}$ (Å)	27.2 ± 4.8
weight average apparent persistence length $L'_{T,w}$ (Å)	24.2 ± 1.5
Z average apparent persistence length $L'_{T,z}$ (Å)	23.0 ± 0.6
weight average reduced viscosity $[\eta]$ (cm ³ g ⁻¹)	127.0 ± 9.6
overlap concentration (c^*) (10^{-3} g cm ⁻³)	7.87 ± 0.59

^a Attempting to estimate the true persistence length L_T by removing excluded volume effects lead to a value of about 15 Å.

Figure 1 shows the concentration distribution of the PVP, represented as $C(M)$, where $C(M) dM$ is the concentration of polymer whose molecular weight is contained in the mass interval M to $M + dM$. Also shown are the corresponding root-mean-square radius of gyration and intrinsic viscosity (actually reduced viscosity at very low concentration) distributions, $R_g(M)$ and $[\eta](M)$, respectively. Table 1 summarizes the relevant average masses, radii of gyration and viscosity. It is of concern that the polydispersity of the sample is fairly high; $M_z/M_w = 1.64$ and $M_w/M_n = 1.79$. This is a potential complication in the interpretation of batch light scattering data, for which M_w alone is measured in the limit of $q = 0$. To assess flexibility, the apparent persistence length L_T' is also shown in Table 1, where the long chain limit relates this to the mean square radius of gyration $\langle S^2 \rangle = R_g^2$, and the polymer contour length L , via $\langle S^2 \rangle = LL_T'/3$.

The so-called semidilute regime is that range of concentrations for which the polymers interpenetrate. The concentration at which this begins to happen is denoted c^* , below which the polymers are in the dilute range of concentration. Since the inverse of the intrinsic viscosity, $[\eta]^{-1}$, is the mass per unit of hydrodynamic volume for a single polymer, the approximation $[\eta]^{-1} = c^*$ is often used. We measure $[\eta] = 127$ cm³ g⁻¹, giving $c^* = 8 \times 10^{-3}$ g cm⁻³, which corresponds to $[PVP] = 0.069$ M. (Note that this last concentration refers to the concentration of PVP monomers. Using a number-average molecular weight of 450×10^3 g mol⁻¹, this corresponds to a molecular concentration of about 18 μM.) All of the data we present were taken with the PVP concentration in the dilute regime.

All aqueous solutions were made starting with doubly distilled, deionized water, from a Modulab Analytical Research Grade ultrafiltered Continental Water System, whose last stage contains a 0.22 μm filter.

Solutions were prepared on the basis of measured, dry weight. Unless otherwise indicated, concentrations of PVP,

POE, and SDS refer to the molar concentration of monomer, whose molar masses are, respectively, 114.11, 44, and 288.4 g/mol.

Static light scattering (SLS) is the principal technique used. SLS measurements were made with a Wyatt Technology Dawn-F DSP light scattering photometer (Santa Barbara, CA). Scintillation vials of 25 mm diameter were used for "batch" measurements of the PVP/SDS aggregates, permitting the scattering to be measured simultaneously from 18 angles from 26 to 145°. Data were transferred via an RS-232c line to a microcomputer. W.R. wrote software for data acquisition and analysis.

Raw scattering voltages at each angle scattering vector q , $V(q)$, were transformed to absolute Rayleigh ratios $I(q)$ according to

$$I(q) = \frac{V(q) - V_s(q)}{V_a(q_r) - V_d(q_r)} N(q) I_a F \quad (1)$$

where $V_s(q)$ is the pure aqueous solvent scattering voltage at q , $V_a(q_r)$ is the voltage at a reference wavevector q_r (here taken as that corresponding to 90°) of the absolute calibration solvent, toluene, with a known absolute Rayleigh scattering ratio for 633 nm at $T = 25^\circ\text{C}$ of $I_a = 0.00001408\text{ cm}^{-1}$. $V_d(q_r)$ is the photodetector dark count at the reference wavevector. F is a geometrical correction factor which, for the upright cylindrical batch cells used, amounts to the squared ratio of the refractive index of the sample's solvent to that of toluene divided by the total Fresnel reflection losses at the glass/solvent interface. The scattering vector q has its usual definition as

$$q = (4\pi n/\lambda) \sin(\theta/2) \quad (2)$$

where n is the index of refraction of the solvent, λ is the vacuum wavelength of the laser and is the scattering angle. $N(q)$ is the normalization factor for each photodiode which is computed according to

$$N(q) = \frac{V_n(q_r) - V_s(q_r)}{V_n(q) - V_s(q)} \quad (3)$$

where $V_n(q_r)$ is the scattering voltage of the normalization solution in the sample's solvent at the reference wavevector (corresponding to $\theta = 90^\circ$). The normalization solution is composed of an isotropic scatterer in the sample's solvent. In this case an aqueous solution of dextran of $M_w = 15\text{ kD}$ was used at a concentration of 12 mg/mL.

The standard Zimm single contact approximation for a single component system was used for analyzing the total Rayleigh ratios. In the limit $q^2 \langle S^2 \rangle < 1$, this is expressed as

$$\frac{Kc}{I(q)} = \frac{1}{M_w} \left(1 + \frac{q^2 \langle S^2 \rangle_z}{3} \right) + 2A_2c \quad (4)$$

K is an optical constant, given for vertically polarized incident light as

$$K = \frac{4\pi^2 n^2 (\partial n / \partial c)^2}{N_A \lambda^4} \quad (5)$$

N_A is Avogadro's number and $\partial n / \partial c$ is the refractive index increment of the solution per unit mass concentration increase of polymer. Values for dn/dc of PVP were taken from ref 35 at $T = 25^\circ\text{C}$, and extrapolated to $\lambda = 633\text{ nm}$ (the extrapolated values are only slightly different than those at lower wavelengths). For PVP, $dn/dc = 0.173$; for POE, $dn/dc = 0.135$. For SDS, at $\lambda = 436\text{ nm}$, $dn/dc = 0.121 - 0.0022 C_s(M)$,³² and was found independently in our laboratory to be 0.113 at $\lambda = 633\text{ nm}$.

All measurements were carried out at 25°C .

Scattering from a Multicomponent System

Since we are interested chiefly in static scattering from a multicomponent system, consider the general expression for the excess scattering (i.e. total scattering minus solvent scattering background) for a system of r components³³

$$I(q) \propto \sum_{i,j=1}^r a_i S_{ij}(q) a_j \quad (6)$$

where a_i is the differential refractive index (or optical contrast factor) for species i , given by $a_i = (\partial n / \partial c)_i$. The S_{ij} terms are the partial structure factors given in matrix form by³⁴

$$S_{ij} = \delta_{ij} + (N_i N_j)^{1/2} \int [g(\vec{r}_{ij}) - 1] e^{i\vec{q} \cdot \vec{r}_{ij}} d^3 r_{ij} \quad (7)$$

where N_i and N_j are the particle densities of species i and j , respectively, and $g(r_{ij})$ is the interparticle correlation function, given by

$$g(r_{ij}) = \exp[-U(r_{ij})/kT] \quad (8)$$

$U(r_{ij})$ is the potential of mean force between particles i and j separated by a center-to-center distance r_{ij} . If the interactions between two different species are repulsive, then $S_{ij} < 0$ (recall $\delta_{ij} = 0$, for $i \neq j$), and the total scattering will be less than the sum of the total scattering of the individual species. Similarly, for attractive interactions between different species, the total scattering will be greater than the sum of the individual scattering, whereas for zero or negligible interactions, the total scattering should be just the sum of the individual species' scattering.

For the case at hand we assume, with experimental justification, that the only entities which scatter significantly are bare polymers (when no SDS is added), polymer/micelle aggregates, and free micelles. Individual surfactant molecules and counterions in solution are assumed to scatter negligibly. Furthermore, we ignore polymer polydispersity, as well as variations in surfactant/polymer ratios in S/P assemblies, and consider that we are measuring a weight-average of the assemblies. The excess scattering (expressed in terms of the Rayleigh scattering ratio) is then

$$I_{\text{total}}(q) = S_{aa}(q) P_a(q) K_a c_a M_a + 2S_{am}(q) [K_a c_a M_a K_m c_m M_m P_a(q) P_m(q)]^{1/2} + S_{mm}(q) P_m(q) K_m c_m M_m \quad (9)$$

where the "a" subscripts refer to the P/S assemblies, and "m" subscripts refer to the micelles free in solution.

Because both PVP/SDS aggregates and free SDS micelles are negatively charged (as demonstrated in the accompanying paper) their interaction is repulsive, and we expect $S_{am}(q)$ to be negative, and, at low solute concentrations, negligible. Hence the scattering we measure in a mixture of SDS/PVP aggregates and SDS micelles at given concentrations would be less than or equal to the sum of the scattering from individual SDS/PVP and SDS micelle populations at the given concentrations. We therefore expect the total scattering from a solution of PVP/SDS to be that due to the PVP/SDS

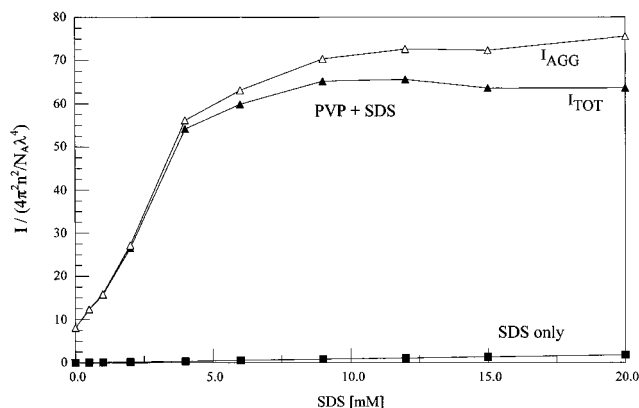


Figure 2. Scattering (divided by polymer independent quantities) vs [SDS], with and without PVP. From bottom to top: pure SDS, I_{tot} is measured scattering for PVP/SDS mixtures, and I_{agg} is the computed scattering due solely to the PVP/SDS aggregates, according to the procedure and assumptions described in the text. The observed total scattering is approximately equal to the scattering from just the PVP/SDS aggregates.

aggregates, minus the second (interaction) term in eq 9, plus a small term due to free SDS micelles.

By subtracting off the scattering due to pure SDS at a given concentration from that of a PVP/SDS solution at the same [SDS], we necessarily obtain a least lower bound on the component of scattering from the PVP/SDS aggregates alone since, for a given concentration of SDS, the number of free micelles is less in a solution with PVP, reducing the micelle-only term in eq 9.

Results and Analysis

Demonstration that the Majority of Scattering Is from PVP/SDS Aggregates. The SLS data presented below measure $I_{\text{total}}(q)$ as expressed by eq 9. We are chiefly interested, however, in characterizing the behavior of the PVP/SDS aggregates, so it is important to assess what fraction of $I_{\text{total}}(q)$ is due only to scattering from these latter entities. Figure 2 shows $I/(4\pi^2 r^2 / N_A \lambda^4)$ (i.e., I divided by polymer independent quantities) extrapolated to $q = 0$ for a PVP concentration of [PVP] = 3 mM, while increasing SDS concentration systematically from 0 to 20 mM. Concentration of salt was [NaCl] = 0.5 M. This combination of low concentration and high added salt serves to minimize A_2 effects. One sees an increase in scattering intensity with increasing SDS concentration until about [SDS] = 5 mM, at which point the scattering saturates sharply and is roughly constant with increasing SDS concentration (we believe this is related to saturation of PVP with bound SDS, which is the so-called polymer saturation point, PSP). Also shown in Figure 2 is scattering from pure SDS, and a calculated curve of scattering from aggregates only (we discuss this calculation below). Equation 9 is simplified by the fact that $P(q=0) = 1$. Further, since for a single scattering species

$$I(q=0) = \frac{KcM_w}{1 + 2A_2M_w c} \quad (10)$$

we can write

$$S(q=0) = (1 + 2A_2M_w c)^{-1} \cong 1 - 2A_2M_w c \quad (11)$$

for both pure PVP and pure SDS. With this in hand,

we estimate the magnitude of the cross term in eq 9. Since we cannot say, a priori, how much SDS remains free in solution, we make the worst case assumption that all of it is (i.e., that no SDS binds to PVP). Finally, we must estimate the interaction term, (i.e., the structure factor), for the two species, $S_{\text{AM}}(q=0)$. The simplest model is that of hard sphere exclusion. That is, $g_{\text{AM}}(r) = 0$ for $r < (R_A + R_M)$, and $g_{\text{AM}}(r) = 1$ for $r > (R_A + R_M)$, where R_A and R_M characterize the exclusion volume of the two species, polymer/micelle assemblies and free micelles. The structure factor is then given by

$$S_{\text{AM}}(q=0) = -(N_A N_M)^{1/2} \frac{4\pi}{3} (R_A + R_M)^3 \quad (12)$$

Since the micelles are actually well approximated as a sphere, we take their radius, ~ 20 Å, as their exclusion radius. For the polymer chains, the choice of R is not so straightforward. Obvious choices for the exclusion radius are the radius of gyration, R_g , and the hydrodynamic radius, R_h . However, the radius of gyration characterizes the distribution of mass in a polymer and may in fact have nothing to do with excluded volume. Similarly, the hydrodynamic radius characterizes interactions of the polymer with solvent, rather than with other solute. We feel that it is more appropriate to use a radius obtained in the following manner. If we model the polymer-polymer interactions as that of hard spheres in eq 7, we can relate the calculated quantity $S(q=0)$, involving an excluded volume, to the experimental quantity A_2 . This relationship is given by

$$S(q=0) = 1 - N_1 \frac{4\pi}{3} (2R)^3 \cong 1 - 2A_2 M_w c \quad (13)$$

from which we obtain the familiar relationship

$$A_2 = 4N_A \frac{4\pi R^3}{3M_w^2} \quad (14)$$

Using $M_w = 801\,000$ g mol⁻¹ and $A_2 = 0.000\,25$ cm³ g² mol⁻¹, we obtain for R a value of approximately 250 Å. We feel that this radius obtained from eq 14 more properly characterizes the volume excluded by the polymer. On the other hand, it is not so clear that a polymer will exclude from a micelle the same volume that it would exclude from another polymer. In fact, this expression probably overestimates the excluded volume interaction of the polymers and micelles. Thus, this also constitutes a worst case assumption. With these considerations, we can extract from eq 9 the scattered intensity due to aggregates only and compare it to the total observed scattering. This comparison is presented in Figure 2. We see that the total scattering is less than the scattering due to aggregates alone, which reflects the suppression of scattering due to repulsive interactions between the two species. At worst, the suppression is about 20% for [PVP] = 3 mM. In the more interesting region below about [SDS] = 5 mM (which reflects increasing SDS binding), the deviation is less than 10%. Thus, it is seen that the majority of the scattering is due to the PVP/SDS aggregates. Since the computed line shown takes the "worst case" that no SDS binds at all, and are obtained with what is probably a large overestimate of the exclusionary interaction, the actual light scattered by the PVP/SDS

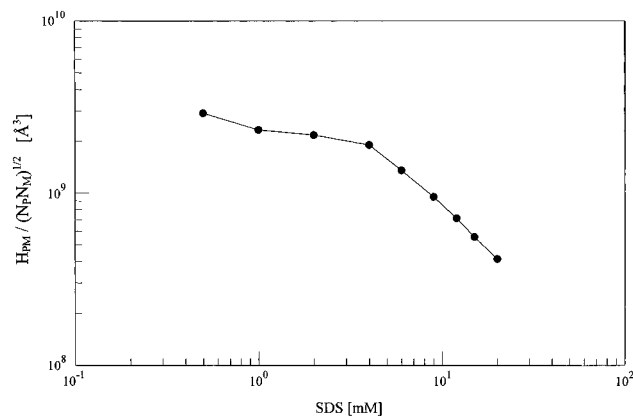


Figure 3. H_{PM} vs SDS obtained from aggregate scattering, as described in the text. N_P and N_M are number densities of PVP and SDS, respectively.

aggregates is probably much closer to the total observed scattered light.

With this determination, we henceforth approximate the total observed scattering as the scattering solely from the PVP/SDS aggregates.

Estimate of Binding Parameters from the Multicomponent Scattering Model. The model of scattering from multicomponent systems also permits us to evaluate the binding energy and binding volume of the polymer/surfactant aggregates. This is done in the following manner. If we express eq 6 in terms of the micelles and bare polymers rather than as polymer/micelle aggregates and free micelles, then the model predicts that the attractive interaction between the polymers and the surfactant molecules will be reflected in the cross term. In other words, the scattering of the aggregates, which we assume is equal to the total scattering, can be expressed as three terms: scattering from polymers only, scattering from micelles only, and scattering due to a cross term with an attractive structure factor. If we neglect the effects of the polymer and micelle A_2 (i.e., we assume S_P and S_M are 1) and denote this attractive structure factor as H_{PM} , we can calculate $H_{PM}/(N_P N_M)^{1/2}$ (which should be independent of concentration) from eq 6 as

$$\frac{H_{PM}}{\sqrt{N_P N_M}} = \left(\frac{1}{\sqrt{N_P N_M}} \right) \left(\frac{I_{TOT} - I_P - I_M}{\sqrt{I_P I_M}} \right) \quad (15)$$

where I_{TOT} is the total observed scattering, I_P is the scattering due to polymers alone, and I_M is the scattering due to surfactant micelles alone. This calculation, using the data in Figure 2, is shown in Figure 3. Note that since the scattering in Figure 2 is extrapolated to $q = 0$, the structure factor shown in Figure 3 is $H_{PM}(q = 0)$. The data are somewhat noisy (due primarily to the noise in I_M , which shows up in the divisor of eq 15), but certain trends are clear. We see that H_{PM} is roughly constant with [SDS] until the saturation point is reached and then falls with [SDS] as $[SDS]^{-1}$. Using eq 7, we can relate the H_{PM} obtained from the data to the polymer/micelle binding energy using

$$\frac{H_{PM}}{\sqrt{N_P N_M}} = \sum_0^{\infty} (g(\mathbf{r}) - 1) d^3 \mathbf{r} \quad (16)$$

where $g(\mathbf{r})$ is the two particle correlation function for

the two species. If we assume a spherically symmetric square well attraction for which $U = -U_B < 0$ for $r < R$ and $U = 0$ for $r > R$, then eq 16 becomes

$$\frac{H_{PM}}{\sqrt{N_P N_M}} = (\exp(U_B/k_B T) - 1) \frac{4\pi R^3}{3} \quad (17)$$

The only data from Figure 3 which satisfies the assumption of constant $H_{PM}/(N_P N_M)^{1/2}$ is the low concentration data below saturation. Using only this region in eq 17, we obtain

$$\frac{H_{PM}}{\sqrt{N_P N_M}} = (\exp(U_B/k_B T) - 1) \frac{4\pi R^3}{3} \approx (2.33 \pm 0.43) \times 10^9 \text{ Å}^3 \quad (18)$$

With only one data value and two independent parameters, we cannot solve unambiguously for the binding energy, U_B , and range of attraction, R , but we may estimate the binding energy by considering some reasonable ranges. One possibility is that the attraction is weak and the micelles are constrained over a range of the order of the radius of gyration. Using this in eq 18, we obtain $U_B/k_B T = 0.90 \pm 0.17$, a comparatively weak binding energy, but sufficient to bind significant amounts of SDS to the PVP. Such a weak binding energy is consistent with the observation that a large fraction of added SDS remains free in solution. Another possibility is that the attraction is short range and only extends over the size of a micelle, roughly 20 Å. This gives $U_B/k_B T = 11.15 \pm 2.06$, which is quite a strong binding energy. For this to be consistent with the large amounts of free SDS, it would be necessary that the entropy costs of binding be comparably high. We address this point later when we approach the binding of SDS to PVP from a thermodynamic perspective. Finally, one could imagine a very short range interaction, affecting only surfactant molecules within a few angstroms of the polymer (this is a common picture). Using $R = 3$ Å, we obtain $U_B/k_B T = 16.84 \pm 3.11$; again, this is quite a strong binding. The concerns about entropy costs expressed above apply here. Thus, for any reasonable range of attraction, the two-component scattering model predicts moderate to strong binding. The value predicted is seen to be quite sensitive to the range assumed, which is itself uncertain. On the other hand, the values we find from this model of light scattering are in accord with the values we determine later using a thermodynamic model of SDS/PVP binding.

Zimm Plot Determinations. Obtaining conventional Zimm plots for the SDS/PVP system is complicated by the existence of multiple equilibria of SDS between aggregates with PVP, free micelles, and free monomers, as well as variations in total solution ionic strength as [SDS] is changed. When total solute concentration is decreased using a fixed ionic strength solution for dilution, and [SDS]/[PVP] is kept constant, ionic strength decreases, and care must be taken when crossing the polymer saturation point (PSP) and the CAC. In the next section, we discuss how the data from the Zimm plots is analyzed to determine the fraction of added SDS which is bound and to obtain the molecular weight, radius of gyration, and second virial coefficient.

Evaluation of Binding Fraction, Aggregate Molecular Weight, and Density of Binding States. Using Equation 4, the Zimm equation expresses the

scattering intensity from the polymer/surfactant aggregates as

$$\frac{K_{\text{AGG}} c_{\text{AGG}}}{I(\theta)} = \frac{1}{M_{\text{AGG}}} \left(1 + \frac{\langle S^2 \rangle_z q^2}{3} \right) + 2A_{2,\text{AGG}} c_{\text{AGG}} \quad (19)$$

However, since we assume that the fraction, f , of dissolved surfactant actually bound to the polymer chains is a priori unknown, the mass concentration of aggregate, c_{AGG} , and the constant K_{AGG} (which contains the material-dependent quantity dn/dc_{AGG}) are also unknown, and so it is impossible to use eq 19 to obtain the aggregate molecular weight. However, the mass concentration of bound SDS is given by $fM_s N_s$, where M_s is the molecular weight of a surfactant molecule and N_s is the density of surfactant molecules. On average, the total mass bound to each polymer chain is $fM_s N_s / N$, where N is the density of polymer chains. The total mass of the aggregate is the sum the bare polymer chain mass, M , and the surfactant bound to each chain, or

$$M_{\text{AGG}} = M + fM_s N_s / N = M \left(1 + f \frac{c_s}{c} \right) \quad (20)$$

where the relations $c = MN$ and $c_s = M_s N_s$ have been used. Again, using the approximation that all scattered light is due to the aggregates (i.e., that the unbound surfactant does not significantly scatter light) and that the number of aggregates is the same as the number of polymers, we can use the fact that $c_{\text{agg}}/M_{\text{agg}} = N_{\text{agg}} = N = c/M$ and eq 2 to conclude that the weight concentration of scattering material is

$$c_{\text{AGG}} = c + fc_s = c \left(1 + f \frac{c_s}{c} \right) \quad (21)$$

Finally, we obtain the refractive index increment of the aggregates by assuming that the index change caused by a micelle is the same whether bound to a polymer or free in solution. This is equivalent to assuming that the dielectric susceptibility of surfactants and polymer to the incident electric field is unchanged by their state of association. In the unassociated state, the refractive index increments are measured to be $(dn/dc)_{\text{SDS}} = 0.113 \text{ cm}^3/\text{g}$ and $(dn/dc)_{\text{PVP}} = 0.173 \text{ cm}^3/\text{g}$. The total index change produced by the polymer and bound surfactant is $\Delta n = c(dn/dc_p) + f_s(dn/dc_s)$. Assuming $(dn/dc_{\text{AGG}}) \approx \Delta n/c_{\text{AGG}}$, we get

$$\left(\frac{dn}{dc} \right)_{\text{AGG}} = \left(\frac{dn}{dc} \right)_p \frac{\left(1 + f \frac{c_s(dn/dc_s)}{c(dn/dc_p)} \right)}{\left(1 + f \frac{c_s}{c} \right)} \quad (22)$$

Using eqs 20 through 22, we may recast eq 19 in the experimentally more useful form

$$\frac{Kc}{I(\theta)} = \frac{1}{M \left(1 + f \frac{c_s(dn/dc_s)}{c(dn/dc_p)} \right)^2} \left(1 + \frac{\langle S^2 \rangle_z q^2}{3} \right) + 2A_{2,\text{AGG}} \left(1 + f \frac{c_s(dn/dc_s)}{c(dn/dc_p)} \right)^2 c \quad (23)$$

Thus, the Rayleigh ratio allows the determination of the

Table 2. Zimm Plot Results for PVP/SDS Aggregates (Ratio [PVP]/[SDS] = 1.0)

NaCl concentration [mM]	0.010	0.050	0.500
f	0.124	0.508	0.725
molecular mass (10^3 g mol^{-1})	1152	2003	2486
radius of gyration (\AA)	698	745	523
second virial coefficient ($10^{-4} \text{ cm}^3 \text{ mol}^{-2}$)	4.65	2.14	0.694

binding fraction and thus the aggregate mass, as well as the radius of gyration and the second virial coefficient. Note that the first term on the right in eq 23 does not give the aggregate mass directly. Note also that the second virial coefficient appearing in eqs 19 and 23 is that for the aggregate, and will generally be an unknown function of bound surfactant. To determine $A_{2,\text{AGG}}$, Zimm plots were performed in which the dilution was performed while maintaining a fixed ratio of total surfactant to polymer density. This provides the apparent mass

$$M_{\text{APP}} = M \left(1 + f \frac{c_s(dn/dc_s)}{c(dn/dc_p)} \right)^2 \quad (24)$$

from which the binding fraction, f , and the actual aggregate mass, $M_{\text{W,AGG}} = M(1 + f_s/c_p)$ are obtained. The Zimm plots provide the correct radius of gyration since this is independent of M_{W} , A_2 , and dn/dc ; and an apparent second virial coefficient which is related to the actual virial coefficient by

$$A_{2,\text{APP}} = A_{2,\text{AGG}} \left(1 + f \frac{c_s(dn/dc_s)}{c(dn/dc_p)} \right)^2 \quad (25)$$

Using the f obtained from the mass determination, the conversion to the actual A_2 is straightforward. The actual molecular weight of the aggregate, the binding fraction, the radius of gyration, and the second virial coefficient obtained from Zimm plots are all presented in Table 2. The pronounced drop in $A_{2,\text{AGG}}$ is consistent with the fact that the mass increases significantly while the radius of gyration remains relatively constant. Also observed is a weak variation in R_g with added salt. While consistent with the results of Gilyani et al.,⁷ this is somewhat surprising, since it implies that there is no strong interaction between the electrically charged micelles on the same polymer.

For sufficiently high salt, which minimizes A_2 , and a sufficiently small polymer concentration, the last term in eq 4 can be ignored and the apparent mass can be read directly from the intercept of Kc/I . Doing so with the data of Figure 2 allows us to determine f as a function of added SDS (recall that [PVP] and [SDS] refer to the polymer monomer and SDS molecule concentrations). This is plotted in Figure 4 as a log-log plot, where the ordinate is the SDS molecule number density normalized to the PVP monomer number density. We see that the fraction of surfactant bound is fixed until $[\text{SDS}]/[\text{PVP}] \approx 1.3$. Zanette et al.¹⁶ find that the polymer saturation point (PSP) occurs when $[\text{SDS}]/[\text{PVP}] \approx 0.3$ for both poly(vinylpyrrolidone) and poly(ethylene oxide), when the polymer masses are 40 000 and 10 000, respectively. If we identify our binding saturation point with their PSP obtained in conductivity measurements, this suggests a weak dependence of the saturation point with polymer mass (a factor of 4.3 increase in $[\text{SDS}]/[\text{PVP}]$ for a factor of 22 increase in molecular weight). The average f in the constant

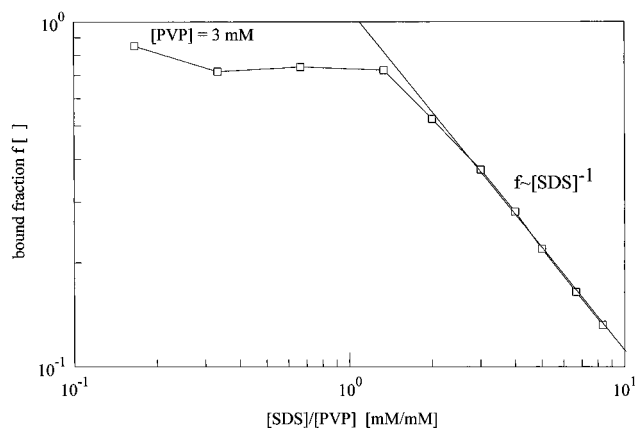


Figure 4. Bound fraction of SDS, denoted f , vs $[SDS]/[PVP]$ for $[PVP] = 3\text{ mM}$.

(i.e., low $[SDS]$) region is 0.77 ± 0.03 . We estimate that the effect of A_2 on these results is no more than 20% and most likely under 5%. Above this constant region, the value of f decreases with increasing $[SDS]$ as $f \sim [SDS]^{-1}$. That is, in this region, the density of bound surfactant, $f[SDS]$, is fixed at its saturated value. Using only data for which $[SDS]/[PVP] > 2$, we obtain $f[SDS] = 3.32 \pm 0.038\text{ mM}$. If we interpret this to mean that there are a fixed number of sites on each polymer onto which a surfactant molecule may attach, then we may evaluate this number of sites. Expressing it as the number, r , of sites per polymer monomer, and dividing the total density of bound surfactant by the density of monomers, we obtain $r = f[SDS]/[PVP] = 1.11 \pm 0.01$. With this number of sites, we expect the bound surfactant to saturate (and thus f to begin to decrease as $f \sim [SDS]^{-1}$) when the bound surfactant, $f[SDS]$, equals the density of binding sites, $r[PVP]$. Using the low $[SDS]$ value of f , saturation should occur when $[SDS]/[PVP] \cong r/f = 1.46$ very near the observed saturation value of $[SDS]/[PVP] = 1.3$. Furthermore, if we again identify the elbow in the plot of f vs $[SDS]$ as the PSP, we can express the number of sites per monomer, r , as $r = f_{[SDS] < PSP} [PSP]/[PVP]$, where $f_{[SDS] < PSP}$ refers to the constant value of f for concentrations of SDS below the PSP.

Finally, we can estimate the average linear charge density along the polymer chain. This is given in elementary charges per Bjerrum length by

$$\lambda = \alpha r \frac{0.72\text{ nm/Bjerrum length}}{0.256\text{ nm/monomer}} = \alpha f_{[SDS] < PSP} \frac{PSP}{[PVP]} (2.81) \quad (26a)$$

where α is the fraction of bound SDS that are ionized. Assuming the fraction ionized is¹⁶ 0.30 and $f_{[SDS] < PSP} = 0.77$, we have 0.84 elementary charges per Bjerrum length at high salt for $[PVP] = 3\text{ mM}$. This suggests that the saturation of SDS attaching to the PVP chains may be dictated by the requirement that there be less than about one elementary charge per Bjerrum length, strongly reminiscent of Manning condensation. A telling test of this interesting notion would consist of determining αr under different conditions (different ionic strength, varying polymer molecular weight) and determining if the PSP in fact correlates with a linear charge density under one elementary charge per Bjerrum length. Figure 5 shows that f decreases strongly with decreasing C_s .

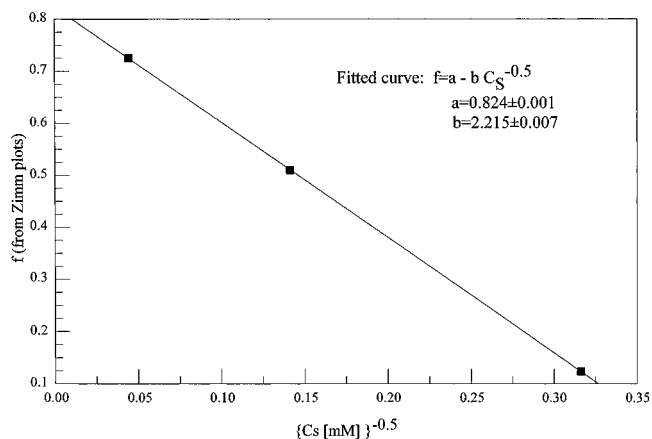


Figure 5. Bound fraction of SDS, denoted f , as a function of $(C_s)^{-1/2}$ from Zimm plots with an empirical linear fit.

A particular concern here in considering f is that the α used was measured at very low ionic strength and there is no reason to suppose that it would be independent of ionic strength. In fact, a simple mass action argument suggests that as the Na concentration increases through adding salt, α would decrease. For this interpretation of SDS saturation to hold, it would be necessary that the product $\alpha f_{[SDS] < PSP}$ be independent of added salt, since it is observed that $PSP/[PVP]$ is very weakly dependent on added salt. We discuss this further in the accompanying paper on polyelectrolyte properties, but briefly we do see evidence that the product $\alpha f_{[SDS] < PSP}$ is independent of added salt (although at a value lower than seen here, reducing the inferred linear charge densities by about a factor of 3). Together with the observed increase of f with $[NaCl]$ (see Table 2), this suggests that α decreases dramatically with added salt, as might be suspected from the mass action argument. However, the reduction in screening and attendant increase in electrostatic potential caused by reduced salt concentration could be expected, at sufficiently small added salt, to decrease α . It is therefore possible that these two competing effects produce a peak in α as a function of added salt.

Thermodynamic Model. Light scattering reveals that a significant fraction of micelles do not bind to the PVP polymers, so that the free energy difference between bound and free states cannot be very large. Furthermore, to within experimental error, f is constant as the ratio of $[SDS]/[PVP]$ increases (below the PSP), suggesting the micelle binding is not cooperative and that there is a certain mean potential all micelles bound to a polymer experience. A priori this potential could be shallow and broad or deep and narrow.

We would, in fact, like to estimate the magnitude of the binding potential U_B of a micelle to a polymer, knowing the experimentally determined fraction of bound micelles f . A simple model is to focus on the micelles and consider them in one of two phases: bound to polymer or unbound in solution. We do not explicitly treat the equilibrium conditions between surfactant monomers and the micelles, whether bound or free, since we are chiefly interested in the surfactant concentration zone above the CAC and below the PSP, where the primary effect of adding surfactant to the solution is to increase the total number of micelles, which are divided among the bound and unbound phases. We consider the same number of micelles to be bound, on average, to each polymer molecule, so that

above the CAC there are no free polymers. Also, considering that the solvent domain of random coil polymers such as PVP is quite large, we do not distinguish between water "within" the polymer coil, nor that in the bulk. Hence, we can seek an expression for f by setting equal the chemical potential of the micelles in each phase. Equivalently, we can utilize the standard Boltzmann weighting for the free and bound states, designated states 1 and 2, respectively. That is

$$n_2 = n_1 \frac{g_2}{g_1} \exp[-(U_2 - U_1)/kT] \quad (26b)$$

where g_2 and g_1 and U_2 and U_1 are the degeneracies and energies of the respective states. We take any interactions in the free state to be negligibly small, so that $U_1 = 0$, and denote the energy of the bound state as $U_B (=U_2)$.

Now the degeneracies of each state are related to the number of spatial states available to the micelles. We take the very simple approach here that the ratio g_2/g_1 is simply the ratio of the bound state to free state volumes, V_B and V_F . The definition of what constitutes the bound state volume is the key physical concept here, but as in the two-component scattering formalism, it is not obvious what this volume corresponds to. Before broaching this question, we give the formal relationships involved. Namely, since the bound fraction f is given by

$$f = n_2/(n_1 + n_2) \quad (27)$$

we have, using $g_2/g_1 = V_B/V_F$, and the fact that, per unit volume, $V_B + V_F = 1$

$$f = \frac{1}{1 + \frac{1 - V_B}{V_B} \exp(U_B/kT)} \quad (28)$$

The bound volume might be conceived in at least three different ways: (i) as related to some average volume occupied by a complete polymer, in which case the micelles are only loosely bound to the polymer, but preferentially remain within a polymer's "domain"; which is a model for a shallow, broad potential well; (ii) as related to the micelle volume itself if the micelle is fairly tightly bound to the polymer, which gives a deep, narrow well; or (iii) as an effective volume, involving the volume of several polymer subunits, over which the polymer/micelle interaction occurs, giving an even deeper, narrower well.

In the first case, where the polymer volume defines V_B , we might take a measure of individual polymer volume as $(4/3)\pi R_g^3$, where R_g is the radius of gyration. Using C_p as the polymer concentration in g/cm³ then gives

$$V_B = (4/3)\pi R_g^3 C_p N_A / M \quad (29)$$

where M is the mass of the polymer. R_g is related to M by

$$R_g = aM^b \quad (30)$$

where, for example, $b = 0.5$ for an ideal random coil, nearly 0.6 for a coil with excluded volume, 1 for a rod, and so on. Then

$$f = \frac{1}{1 + \left(\frac{3}{4\pi a^3 M^{3b-1} C_p (g/cm^3) N_A} - 1 \right) \exp(U_B/kT)} \quad (31)$$

from which it can be seen that, for $b > 1/3$, f decreases with decreasing M , assuming that U_B is independent of M . Using the experimentally determined value of $f = 0.7$, and taking typical values of $R_g = 500$ Å, $C_p = 1.14 \times 10^{-3}$ g/cm³ (for [PVP] = 3 mM), and $M \sim 10^6$ yields a binding energy of $U_B = -1.42kT$. Note that this is comparable to the value determined from the two-component scattering model under similar assumptions. Taking $b = 0.5$ gives, for a PVP polymer of $M = 10^4$, $a \sim 0.5$, and $R_g \sim 50$ Å and the same C_p and U_B , $f = 0.128$ for the fraction of bound micelles. Much previous work shows, however, that binding to small polymers (e.g., of $M \sim 10^4$, that is, 100 times smaller than the PVP for the main portion of this work) is also quite strong. It is hence unlikely that V_B is determined by total polymer volume as given by $(4/3)\pi R_g^3$. An experimental test of the dependence of f on M would be nonetheless desirable.

The second viewpoint mentioned is that the binding volume is on the order of the micelle volume itself, v_m , and that a certain number of the polymer's monomers, n_B , constitute a binding site. Then the total binding volume per unit volume is

$$V_B = N_p v_m / n_B \quad (32)$$

where N_p is the number density of the polymer's monomers. Then

$$f = \frac{1}{1 + \left(\frac{n_B}{C_p (mM) N_A v_m 10^{-6}} - 1 \right) \exp(U_B/kT)} \quad (33)$$

where C_p is the millimolar monomer concentration. Using typical values of a radius of 20 Å for SDS micelles and a saturation value of 1.3 PVP monomers/SDS monomer and assuming there are about 80 SDS monomers per micelle give a rough value of $n_B = 100$, as the number of the polymer's monomer per bound micelle. It is not necessary that all these monomers be involved in binding the micelle, as some may merely act as spacers. For $f = 0.7$ this yields $U_B = -8.3kT$, which is a fairly deep attractive well. Again, the thermodynamic approach gives results comparable to those of the two-component scattering model. Since the effective free energy difference is only about $-kT$, the entropic penalty for a micelle binding to a polymer is quite high, nearly as high as the well is deep.

This latter computation suggests that the attractive wells are deep but short range. A bound polymer could be expected to stay bound to a particular polymer site, and not wander about much. In this sense, the models suggested by Cabane,¹⁰ based on neutron scattering, and Dubin,¹¹ in which micelles are actually sort of "wrapped up" by polymer, appear to be reasonable. In the simplest picture of wrapping, the upper bound on elastic energy penalty for a polymer of persistence length L_p per circular turn is given by $kT(L_p/2\pi R) \approx 0.19kT$, using the weight-average persistence length from Table 1 and a micelle radius of 20 Å. Likewise, in a simple three-state rotational isomeric model of a polymer, saying there is only one state which wraps the polymer leads

to an entropy penalty of $kT \ln 3$, or about $1.1kT$ per monomer. This of course is an upper bound, and probably a serious overestimate, as there should be many conformations which allow a polymer to exist on a roughly 3-D spheroidal surface.

In both of the models above, including the third mentioned, f should increase with increasing polymer concentration C_p . It would be desirable to have data on this in the future.

It is still somewhat puzzling that there is no obvious anti-cooperativity of micelles binding to a given polymer. If the intermicellar interactions on a given polymer were strong, one would expect f to decrease with increasing SDS concentration. The flatness of f vs [SDS] may be another indication of the fact that the binding wells are fairly deep and only slightly altered by intermicellar repulsive energy.

Conclusions

Estimates of micelle to polymer binding fraction f as a function of [SDS] and C_s suggest that micelles are bound to polymers in rather narrow, deep wells (several $-kT$), consistent with the picture of their being several or many VP monomers involved for each bound micelle. The large population of free micelles, however, suggests that the net free energy difference is only of the order of kT , suggesting that there is a high entropy cost for binding. The flatness of f vs [SDS] at fixed [PVP] and the relative insensitivity of R_g to bound SDS both suggest an unexpected lack of anticooperativity as successive micelles are bound to a given polymer, which is consistent with the results of Gilyani et al.⁷ The sharp decrease of f with decreasing C_s implies that the well depth may get shallower and/or the binding volume may decrease as intermicellar interactions increase with decreasing C_s .

Equations 28 and 33 give testable predictions of how f should vary with [PVP], and determining how f varies with polymer mass M would give more insight into the nature of the binding volume.

Acknowledgment. The authors acknowledge support for this work from the Louisiana Board of Regents University/Industrial ties program (RDB-11) and from

the Tulane University CPP, supported by the Louisiana Board of Regents and the NSF EPSCOR program.

References and Notes

- (1) Arai, H.; Horin, S. *J. Colloid Interface Sci.* **1969**, *30*, 373.
- (2) Jones, M. N. *J. Colloid Interface Sci.* **1967**, *23*, 36.
- (3) Cockbain, E. G. *Trans. Faraday Soc.* **1953**, *49*, 104.
- (4) Fishman, M. L.; Eirich, F. R. *J. Phys. Chem.* **1975**, *75*, 2740.
- (5) Minatti, E.; Zanette, D. *Colloids Surf. A* **1996**, *113*, 237.
- (6) Goddard, E. D. *Colloids Surf.* **1986**, *19*, 255.
- (7) Gilanyi, T.; Wolfman, E. *Colloids Surf.* **1981**, *3*, 181.
- (8) Chari, K.; Lenhart, W. C. *J. Colloid Interface Sci.* **1990**, *137*, 204; **1990**, *138*, 593.
- (9) Chari, K. *J. Colloid Interface Sci.* **1992**, *151*, 294.
- (10) Cabane, B.; Duplessix, R. *J. Phys.* **1982**, *43*, 1529–1542.
- (11) Dubin, P. L.; Gruber, J. H.; Xia, J.; Zhang H. *J. Colloid Interface Sci.* **1992**, *148*, 35.
- (12) Xia, J.; Dubin, P. L.; Kim, Y. *J. Phys. Chem.* **1992**, *96*, 6805.
- (13) Santos, S. F.; Nome, F.; Zanette, D.; Reed, W. F. *J. Colloid Interface Sci.* **1994**, *164*, 260.
- (14) Winnik, F. M.; Regismond, S. T. A. *Colloids Surf.* **1996**, *118*, 1.
- (15) Ruzza, A.; Froehner, S. J.; Minatti, E.; Nome, F.; Zanette, P. *J. Phys. Chem.* **1994**, *98*, 12361.
- (16) Zanette, D.; Ruzza, A. A.; Froehner, S. J.; Minatti, E. *Colloids Surf.* **1996**, *108*, 91.
- (17) Lewis, K. E.; Robinson, C. P. *J. Colloid Interface Sci.* **1970**, *32*, 539.
- (18) Isemura T.; Imanishi A. *J. Polym. Sci.* **1958**, *33*, 337.
- (19) Karush, F. *J. Am. Chem. Soc.* **1950**, *72*, 2705.
- (20) Tsujii, K.; Takagi, T. *J. Biochem.* **1975**, *77*, 511.
- (21) Fishman, M. L.; Eirich, F. R. *Polym. Repr.* **1969**, *10*, 746.
- (22) Saito, S. *Kolloid Z.* **1967**, *215*, 16.
- (23) Blei, I. *J. Colloid Interface Sci.* **1973**, *43*, 491.
- (24) Yang, J. T.; Foster, J. F. *J. Am. Chem. Soc.* **1953**, *75*, 5560.
- (25) Schwuger, M. J. *J. Colloid Interface Sci.* **1973**, *43*, 491.
- (26) Sartori et al. *Macromolecules* **1990**, *23*, 17.
- (27) Brackman, J. C.; Engberts, J. B. F. N. *J. Colloid Interface Sci.* **1989**, *132*, 250.
- (28) Maltesh, C.; Somasundaram, P. *Langmuir* **1992**, *8*, 1926.
- (29) Maltesh, C.; Somasundaram, P. *J. Colloid Interface Sci.* **1993**, *157*, 14.
- (30) Lissi, E. A.; Albuin, E. *J. Colloid Interface Sci.* **1985**, *105*, 1.
- (31) Norwood, D. P.; Reed, Wayne F. *Int. J. Polym. Anal. Charact.*, in press.
- (32) Hayashi, S.; Ikeda, S. *J. Phys. Chem.* **1980**, *64*, 744–751.
- (33) Benmouna, M.; Vilgis, T.; Hakem, F.; Negadi, A. *Macromolecules* **1991**, *24*, 6418.
- (34) Higgins, Julia S.; Benoit, Henri C. *Polymers and Neutron Scattering*; Clarendon Press: Oxford, England, 1994; pp 119–120.
- (35) *Polymer Handbook*.

MA971318N